Heliyon 10 (2024) e27287

Contents lists available at ScienceDirect

Heliyon

journal homepage: www.cell.com/heliyon

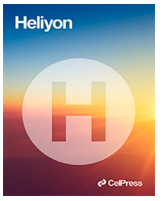

Research article

Experimental investigation on the effect of blending bituminous coal with pinus sawdust on combustion performance parameters

Garikai T. Marangwanda, Daniel M. Madyira *

Department of Mechanical Engineering Science, University of Johannesburg, Johannesburg, South Africa

ARTICLE INFO

Keywords:
Co-combustion
Drop tube furnace
Particle residence time
Bituminous coal
Pinus sawdust
Particle temperature

ABSTRACT

Combustion of bituminous coal and pinus sawdust blends was investigated experimentally within a drop tube furnace (DTF) with the aim of determining particle residence times and temperatures during the process. Evaluation of these parameters gives useful information to engineers who want to optimise the co-combustion process of coal and biomass blends. The DTF experimental approach was used to investigate fuel blends with a pinus sawdust mass substitution of 0, 10, 20, and 30% at different furnace temperatures of 1273, 1473 and 1673 K. Results showed that during stage 1 of the experimental setup which mimics devolatilisation, particle residence time at a distance of 520 mm from the injection point decreased from 0.8 to 0.7 s as blending by pinus sawdust increased from 0 to 30 %. During stage 2 of the experimental setup which mimics char combustion, particle residence time at a distance of 1320 mm from the injection point decreased from 3.9 to 2.0 s as blending by pinus sawdust increased from 0 to 30 %. The blending ratios under investigation demonstrated similar profiles of particle temperature at different furnace positions though further analysis showed that the highly blended samples required less time to attain high temperatures. By extension, since fuel blends with higher percentages of pinus sawdust were able to attain higher temperatures at shorter residence time, combustion intensity was deduced to increase with the blending ratio whilst stability decreased. As such, caution should be taken with materials used for furnace and burner design as high-temperature zones move backwards towards the injection point as blending increases.

1. Introduction

In as much as coal and biomass co-firing results in the reduction of emissions, important combustion parameters such as ignition, burnout, intensity, and stability are influenced as well. Various techniques have been employed in industry to study the effect of fuel blending on combustion parameters, with the most common one being the use of thermogravimetric analysis (TGA) as employed by Marangwanda et al. [1] and others. Unfortunately, short residence times with high heating rates are exhibited by combustion during industrial applications [2,3]. Hence, a drop tube furnace (DTF) becomes indispensable since short residence times (less than 5 s) and high heating rates (between 10^4 and 10^5 K/s) can be achieved and monitored successfully [4].

These combustion parameters are determined experimentally by measuring the primary air flow rate, secondary air flow rate, fuel particle residence time and temperature. Redha et al. [5] used a downfired furnace to demonstrate the positive variation between particle residence time and particle density when solid biomass particles of various densities and aspect ratios are combusted. By use of

* Corresponding author.
E-mail address: dmadyira@uj.ac.za (D.M. Madyira).

https://doi.org/10.1016/j.heliyon.2024.e27287
Received 2 August 2023; Received in revised form 10 January 2024; Accepted 27 February 2024
Available online 6 March 2024

Nomenclature

Units

m	Mass (kg)
c_p	Specific heat capacity (J/kg.K)
T	Temperature (K)
Q	Heat transfer (J)
t	Time(s)
h	Specific enthalpy(J/kg)

Subscripts

p	Particle
rad	Radiation
conv	Convection
w	Wall

Abbreviations

TGA	Thermogravimetric analysis
DTF	Drop tube furnace
CFD	Computational fluid dynamics
HC	Hwange coal
PS	Pinus sawdust

Greek Symbols

Δ	change
ε	emissivity
σ	Stefan Boltzmann constant
λ	Convective heat transfer coefficient

a downfired furnace, Abdul Jameel et al. [6] managed to deduce the relationship between particle residence time and other combustion parameters such as burnout and nitrogen oxide emissions. Extensive work was carried out by Zabrodiec et al. [7] as well to demonstrate how a short residence time during the combustion of biomass results in the rapid release of volatiles, which promotes unstable flames. However, during the co-combustion of coal with biomass, various factors related to the properties of biomass become apparent which makes it difficult to generalise the link between residence time and particle burnout. For example, through computational fluid dynamics (CFD), it has been shown that particle aerodynamics is a function of both particle drag and gravitational properties [5]. Smaller biomass particles exhibit shorter residence times because drag properties are more pronounced in a downfired furnace than gravitational properties (a heavier particle is expected to travel faster as it falls in a downfired furnace). Unfortunately, one of the main limitations of using a DTF is the experimental determination of particle residence time. Combustion within a DTF occurs over short residence times (less than 5 s) hence most researchers employ assumptions based on fluid velocity and fuel particle properties [8,9].

Particle temperature during combustion, particularly after the devolatisation process is mainly dependent on the char particle temperature and the reactions that take place on its surface [10]. Considering the minute size of pulverised particles and the notion that these particles will be in motion during suspension combustion as in the case of a DTF, it becomes difficult to accurately perform experimental measurements. As such, other parameters such as the combustion gas temperature are measured and used to deduce particle temperature [11].

This study focuses on evaluating the combustion parameters of Hwange bituminous coal and pinus sawdust blends undergoing combustion within a DTF. To achieve this, the fuel blends of interest will be physically and chemically characterised, an experimental method compatible with the DTF will be developed, and appropriate methods will be employed to analyse the experimental data. Eventually, a subsequent study that uses this experimental data for validation will be carried out hence producing a CFD model that can be rapidly employed with less cost for optimisation of the co-combustion processes. This study addresses the gap that exists when these combustion parameters are combined whilst optimising the co-combustion process.

2. Background on the use of combustion performance parameters

Optimisation of the blending ratio that can produce the most energy at minimum substitution during industrial co-combustion is an active research area [12]. Some of this research has focused on monitoring the variation of ignition properties during combustion, which is mainly influenced by the variation of particle temperature. On the other hand, combustion properties such as burnout, intensity and stability which are mainly dependent on combustion residence time have also been employed to optimise the co-combustion blending ratio. Ignition refers to the point at which significant burning of combustible matter of fuel begins [13]. By use of image processing techniques, Sarroza et al. [14] associated ignition with flame phenomena and defined it as the point at which a

certain glow is emitted and captured by special cameras during the combustion of a fuel. A less subjective method of defining ignition which is based on TGA analysis has been employed by Wang et al. [15]. These authors preferred to associate the rate of fuel mass loss to ignition. Comparison of ignition temperatures is deemed to be relatively easy thus it is widely used by various researchers when monitoring combustion efficiency. Xing et al. [16] employed a more scientific approach of comparing the ignition index, a derived parameter from ignition temperature and rate of mass loss during combustion. To monitor burnout Priyanto et al. [17] measured the char content at the furnace exit whilst Al-Abbas et al. [18] focused on tracking the char content for each particle within the furnace [19]. As with ignition, TGA as an experimental technique has been employed successfully to monitor fuel burnout with fewer complications [20].

Burnout, a measure used to monitor the level of fuel oxidation, is one of the most common parameters that is investigated during combustion. Conclusions on change in burnout due to blending are mainly based on measuring the carbon in ash content at the exit of the furnace [21,22]. Kruczek et al. [23] reported increased burnout due when hard coal is blended with sawdust biomass. Guo et al. [24] also reported increased burnout whilst investigating the blending of bituminous coal with biomass pellets at a blending ratio of 50% by mass. Pérez-Jeldres et al. [25] did a modelling study on the change in burnout when coal is blended with pine sawdust. Their findings were quite elaborate as they used appropriate CFD techniques such as visualising the contours of burnout rates at different furnace positions. Bhuiyan et al. [26] also employed CFD to demonstrate how burnout increased with biomass blending. As with ignition, a more appropriate parameter called burnout index has also been propounded [27,28]. The main advantage associated with using ignition and burnout indexes as comparative parameters is that they both include appropriate reaction kinetic parameters. As such Jiang et al. [29] reported a gain in burnout index after coal was blended with carbonaceous waste which meant the blended fuel was able to attain complete combustion at lower temperatures.

Another combustion parameter that has been employed when deducing the optimum blending ratio is combustion stability [30]. Stability is commonly linked to the flame behaviour exhibited during the combustion process. Unstable flames can result in poor burnout, flashback flames and unregulated high temperatures that reduce burner integrity [31]. Heat flux meters and infrared cameras are generally employed when performing experimental measurements used to deduce combustion intensity [32]. Ma et al. [10] demonstrated that blending South African coal with either olive waste or wood chips creates zones of high combustion intensity due to high volatile release.

Co-combustion studies which use a DTF to monitor the variation of particle residence time and temperature are limited as most prefer to use the TGA. As such, DTF experimental results related to the fuels of interest to this study have not been reported in literature. This makes the findings of this research important to engineers interested in repurposing coal fired furnaces to become dual fired by use of both coal and biomass, particularly Hwange coal and pinus sawdust.

3. Materials and methods

The characterisation of the fuel blends of interest and subsequent combustion within a DTF was carried out so as to deduce the various combustion parameters.

3.1. Characterisation of fuel blends

The fuels of interest, Hwange coal and pinus sawdust, were prepared according to the requirements of the DTF. To avoid DTF injector clogging, only the particles with a diameter of less than 250 mm were allowed. In general, the diameter of the particles should be less than an eighth of the injector diameter [33]. Data reported in Table 1 summarises the physical and chemical fuel specifications necessary for this current study. Detailed elementary compositions are reported in a previous publication by the same authors [34]. The notation “HC90PS10” is used to represent a sample with 90% Hwange coal and 10% pinus sawdust by mass distribution whilst the notation “SA coal” is used to represent South African coal. Only characterisation relevant to thermal analysis was presented within this study.

Each fuel sample was tested in triplicate for the values of fixed carbon, volatile matter, and ash. As such a standard deviation was determined for each value. Hwange coal exhibited a larger percentage of fixed carbon, ash and bulk density when compared to pinus sawdust. The highest deviation of 1.9680% was experienced when determining the ash content of a HC80PS20 sample. Fortunately, relatively low standard deviations were experienced for most of the values of fixed carbon, volatile matter, and ash. The authors also sought to establish a relationship that can predict the values of fixed carbon, volatile matter, and ash with respect to the percentage of Hwange coal within the fuel blend. With regards to the prediction of fixed carbon, linear regression model produced a line with a coefficient of determination of 0.9906. This meant that for a blending ratio of 95 % Hwange coal, a composition of 52.43 % fixed carbon was expected.

3.2. Drop tube furnace experimental setup

The data given in Table 2 is a summary of the DTF specifications which is a facility that is housed within the ESKOM research and development centre at Rosherville, Johannesburg, South Africa. The detailed furnace components with a corresponding flow diagram of how the DTF operates is given in Fig. 1. The alumina tube within the DTF which is considered to be the furnace had a total height of 2032 mm and an internal diameter of 70 mm. The outer furnace diameter was larger due to the refractory lining made of alumina silicate and heating tubes arranged around the alumina tube.

The fuel blends were introduced using a 2 mm cooled injector at a temperature of 373 K and collected using a 6 mm cooled

Table 1
Chemical properties of coal, pinus sawdust, and fuel blends.[1].

	Proximate analysis[a] (weight %, Standard Deviation)			
	**Fixed carbon	Volatile matter	Ash	Bulk Density (kg/m^3)
HC100	53.97 (0.1326)	23.10 (0.0965)	22.93 (0.0362)	1300
HC90PS10	48.21 (0.8778)	29.91 (0.3786)	21.88 (1.2565)	1210
HC80PS20	46.35 (0.3965)	31.82 (1.5715)	21.83 (1.9680)	1120
HC70PS30	46.02 (0.1113)	33.74 (0.0646)	20.24 (0.1759)	1030
PS100	15.62 (1,3644)	80.68 (1,8058)	3.70 (0,4414)	400
Linear Best Fit	FC = 16.33 + 0.38X	VM = 79.26–0.58X	Ash = 4.407 + 0.20X	
R^2	0.9906	0.9819	0.9678	
SA coal	55.05 (0.2534)	25.02 (0.1753)	19.92 (0.0780)	1300

[a] On a dry basis; ** By difference.

[1] HC: Hwange coal, PS: pinus sawdust, FC: fixed carbon, VM: volatile matter, X: percentage of Hwange coal in fuel blend.

sampling probe at the reactor exit. Within the fuel feeding mechanism, fuel blends weighing 15 g were placed in a test tube connected to the primary carrier gas at an average flowrate of 2.5 NL/min (1.5 < flow rate <3.5). The test tube was placed on a mechanism with an electromechanical vibrator that could be controlled. As such the incoming primary carrier gas fluidised the fuel and transported it into the outgoing pipe leading up to the furnace. The water-cooled sampling probe was maintained at a suction flow rate of between 6 NL/min and 15 NL/min. The secondary gas was preheated to 1273 K for all the cases and the flow rate was set between 10 NL/min and 20 NL/min depending on the furnace residence time that was required.

The collecting probe was set at various predefined distances from the furnace injection point which were 520 mm, 920 mm and 1320 mm along the furnace centreline depending on the experimental procedure as fixed by the operator's manual. The sampling probe was equipped with a bag filter that collected the char or the ash which was analysed accordingly. Three predefined set furnace temperatures as fixed by the operator's manual were investigated which were 1273 K, 1473 K, and 1673 K. These furnace temperatures were used to investigate the effect of particle heating rate on combustion parameters. The injector was assumed to supply a normal to inlet boundary flow direction without any swirl.

The experimental procedure was split into two stages, the first being carried out under a nitrogen atmosphere whilst the second was carried out under an oxygen enriched atmosphere. Limitations around the specified DTF operating temperatures as advised by the manufacturer and plant operator necessitated this procedure of using two stages. Also, the equations used to deduce particle residence time and temperature require an isothermal wall during each experimental run hence both devolatilisation and char combustion required two distinct stages for better analysis. The first stage did not require large residence times thus a 520 mm probing position was sufficient. As such the product of the first stage that could be measured was the solid char since the released volatiles were entrained in the exhaust gases that were not sufficiently monitored. After collecting and testing the char, the second stage then required putting the char within the DTF again under an oxygen enriched atmosphere (3% O_2, 97% N_2) thus producing ash as the final product.

Within a DTF, the fuel sample is subjected to an isothermal heating rate within the range of 10^4 and 10^5 K/s which is quite high when compared to any TGA analysis [3,35,36]. As noted, during the first stage of the experiment which used a nitrogen atmosphere,

Table 2
DTF summarised geometry and operating conditions.

Parameter	Description
Reactor inner diameter	70 mm
Reactor height, total length	2032 mm
Furnace wall temperature settings	1273 K 1473 K 1673 K
Carrier gas	Stage 1 (100% N_2) Stage 2 (3% O_2 97% N_2) 0.25 < Primary flow rate (NL/min)[2] < 0.35 10 < Secondary flow rate (NL/min) < 20 Secondary gas preheated to 1273 K Primary gas at 373 K
Fuel blends	1.5 < flow rate (g/min) < 3.6 373 K

[2] NL/min refers to the flow rate of normal air at 293K and 1.01325 bars in litres per minute.

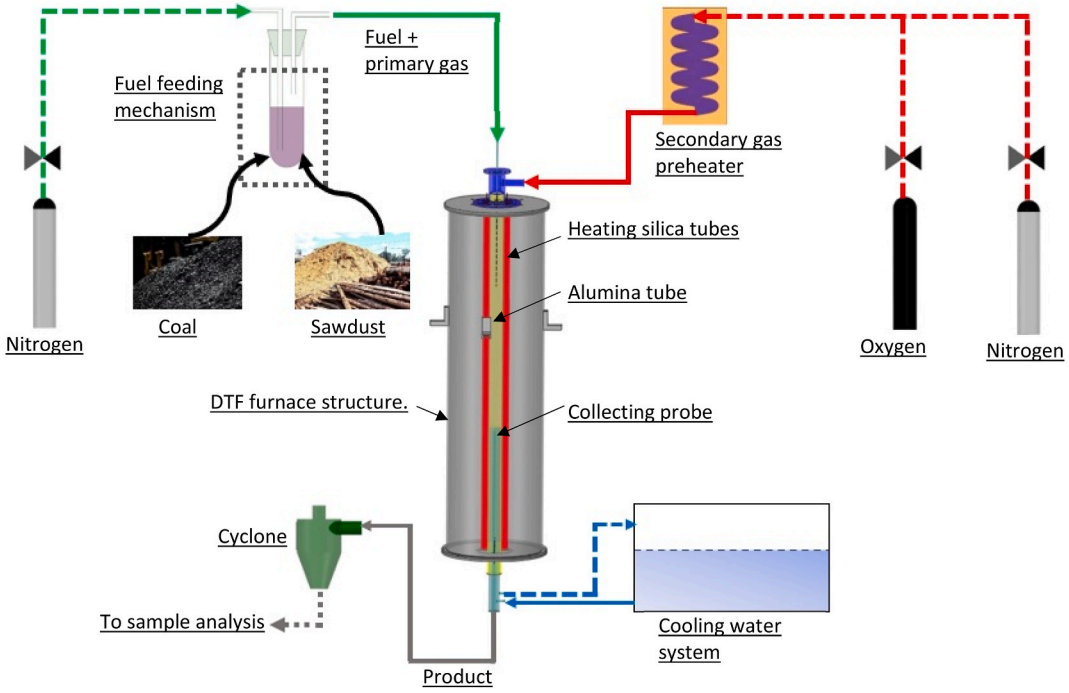

Fig. 1. Flow diagram of the DTF experimental facility.

volatiles were evolved and got entrained in the carrier gas whilst the solid char got collected at the bottom. During the second stage when using an oxygen enriched atmosphere, the char burned out leaving the ash to be collected at the collection probe. Particle properties that could not be measured were determined indirectly based on experimental measurements of various parameters such as fluid velocity and particle size distribution. As such the particle parameters that were evaluated included.

3.2.1. *Particle residence time*

To simplify experimental particle trajectory analysis, a one-dimensional flow was assumed along the furnace axis (z-direction). The particles were assumed to be under the influence of drag based on the Stokes Law and gravitational acceleration. Equation (1) demonstrates how the experimental readings of the carrier gas velocity were used to determine the particle residence time. The Stokes Law was in turn used to determine the terminal velocity of the particles within the DTF.

$$t = \sum_{i=0}^{i=1\text{-}n} \frac{L_i}{v_g + v_t} \tag{1}$$

t:particle residence time (s)
L_i:length of slice (m) *(whole length of DTF was sliced into sections)*
v_g:velocity of carrier gas (m/s)
v_t:terminal velocity of particle (m/s)

3.2.2. *Particle temperature during char combustion*

To determine the experimental particle temperature, it was imperative to acknowledge the conservation of energy and mass as the fuel particle travelled through the furnace. This meant considering all modes of heat transfer as given by equation (2). However, since flow within the DTF was assumed to be one dimensional and the fuel particles were supplied on a dry basis (no vaporisation energy required), a more useful energy balance was formed as represented by equation (3) [37].

$$\frac{d\left(m_p.c_{p,p}.T_p\right)}{dt} = \dot{Q}_{rad} + \dot{Q}_{conv} - \dot{Q}_{vap} \tag{2}$$

$$\frac{h_{reac}.\Delta m_p}{\Delta t} = \dot{Q}_{rad} + \dot{Q}_{conv} \tag{3}$$

m_p:particle mass (kg)
$C_{p,p}$:particle specific heat capacity (J/kg.K)
T_p:particle temperature (K)
$\dot{Q}_{rad}$:Rate of radiation heat transfer (W)

$\dot{Q}_{conv}$:Rate of convection heat transfer (W)
$\dot{Q}_{vap}$:Rate of vaporisation heat transfer (W)
h_{reac}:specific enthalpy of reaction (J/kg)
Δt:residence time (s)

In summary, the left-hand side of equation (3) is reduced to zero when rewritten with assumptions specific to the devolatilisation process. This is because, during devolatilisation, change in combustible mass within the particle tends towards zero for short residence times (char content remains quasi-constant). Concerning stage 2 which symbolises the combustion of char, the energy balance in equation (3) is written to account for the surface reactions taking place on the char surface thus becoming equation (4) [38].

$$\frac{h_{reac}.\left[m_{p,initial} - m_{p,final}\right]}{\Delta t} = \varepsilon.\sigma.A_P.\left(T_p^4 - T_w^4\right) + \lambda.A_P.\left(T_p - T_g\right) \quad (4)$$

h_{reac}:enthalpy of reaction(J/kg) (*Char* + O_2 –> CO_2)
$[m_{p,initial} - m_{p,final}]$:change in mass of combustible matter in char particle (kg)
Δt:residence time (s)
ε:Emissivity
σ:Stefan Boltzmann constant (5.67 × 10-8 W/m^2.K^4)
A:Area (m^2)
w:Wall
g:Gas
λ:Convective heat transfer coefficient (W/m^2.K)

3.2.3. DTF experimental errors

Measurements made by the various instruments during the experiments provided sources for error. All instruments had indications of the possible error which can be considered during analysis of results. The major error which was experienced by the researcher was due to the low collection efficiency of DTF products. However, with regards to DTF measurements the.

- feeding mechanism fluctuated within 1% of the set point due to vibrations of the platform thus flow rates were analysed with a ±0.01 g/min error,
- collecting probe was equipped with a thermocouple having an error percentage of 3% according to the manufacturer,
- carrier gas rotameters had an error of 2% as indicated by the manufacturer.

4. Results and discussion

4.1. Residence time

Before analysing the fuel blends of interest (Hwange coal and pinus sawdust blends), South African coal was used to calibrate the furnace. The particle residence time was indirectly determined through measuring the carrier gas velocity as represented in equation (1). As such the particle residence time is a function of carrier gas velocity, terminal velocity of the particle as well as the position of the particle within the DTF. Concerning South African coal, the residence time during stage 1 which entailed the devolatilisation of the fuel particle is represented in Fig. 2. The furnace temperature was set as 1273 K with the products being probed at 520 mm from the injection point. A linear variation of residence time with position was produced with the error analysis producing values within the 95% confidence band. The residence time at the exit of the furnace was noted to be 1.3 s.

South African coal was also used to calibrate the furnace during the stage 2 experimental setup which involved the combustion of

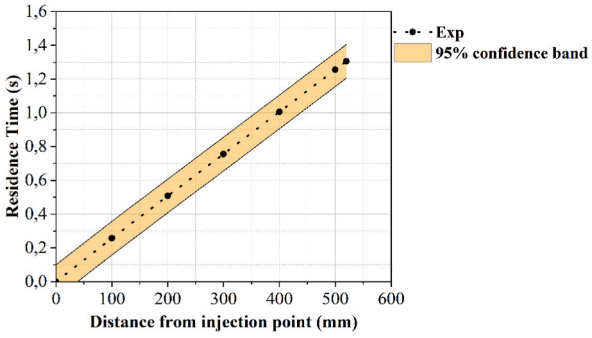

Fig. 2. DTF stage 1 plot of experimental residence times of SA coal fuel.[3]

[3] Exp: represents experimental.

Table 3
DTF stage 2 experimental and predicted residence times of SA coal sample.

Position (mm)	Residence time at various furnace wall temperatures (s)		
	1273K	1473K	1673K
520	1.3	1.1	1.0
920	2.2	1.9	1.7
1320	3.2	2.8	2.5

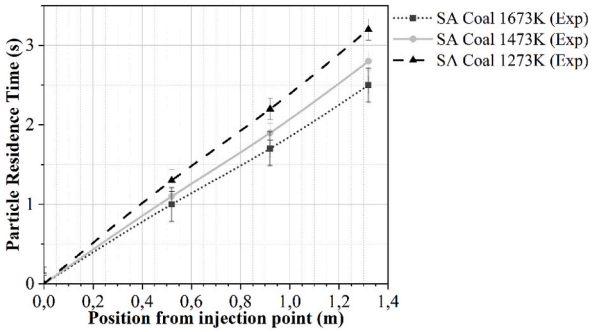

Fig. 3. DTF stage 2 plot of experimental residence times of SA coal fuel.[4]

[4] SA coal: South African coal.

stage 1 products (char) since the atmosphere was enriched with oxygen. The stage 2 setup allowed for extra probing positions at 520, 920, and 1320 mm from the fuel injection point. The stage 2 setup also allowed the researcher to investigate the effect heating rate has on the char particles as they move through the DTF at different furnace wall temperatures of 1273, 1473 and 1673 K. Data obtained on the variation of experimental residence time concerning position is presented in Table 3 and Fig. 3. A linear variation of residence time with position was demonstrated for all the furnace temperatures. Higher furnace temperatures, which resemble higher heating rates resulted in shorter particle residence times. At a position of 1320 mm from the injection point, the particle residence time decreased by 21.88 % as the furnace temperature increased from 1273 to 1673 K with similar trends being exhibited at 520 and 920 mm probing positions. Holmgren et al. [9] found similar relationships between furnace temperature and residence time for both pine stem wood and wheat straw between 1173 and 1373 K during their investigations on the effect of particle diameter and density on combustion within a DTF.

The variation of residence time with position within the DTF for the fuels of interest during stage 1 is shown in Fig. 4. When the products were probed at 520 mm during stage 1 which resembles devolatilisation, blending decreased the residence time from 0.98 to 0.74 s as the ratio of pinus sawdust increased from 10 % to 30 %. A decrease in residence time means the fuel particle is travelling faster within the furnace. Depending on the type of fuel, a residence time variation of 35% from 7.1 to 9.6 s can result in an increase of maximum particle temperature from 975 to 1011 K [5]. A change of maximum particle temperature will result in a change of ignition, combustion stability, burnout, and combustion intensity properties [1]. When Katarzyna [39] performed similar studies on biomass and coal, findings revealed that for large-aspect biomass particles residence time is tremendously influenced by the shape and orientation of these particles. As the fuel particle travels through the furnace, it is under the influence of aerodynamic forces such as gravitational and drag properties. At a furnace temperature of 1273 K during stage 1, Fig. 4 shows that particle residence time is influenced by particle drag properties rather than gravitational properties. As Redha et al. [5] also demonstrated, blending decreases the weight of a fuel particle which in turn reduces the gravitational forces on that particle. Eventually, a lighter particle will require more time to travel a certain distance than a heavier particle. However, in this case, blending with pinus sawdust tends to increase drag forces which makes lighter particles travel quickly within the DTF. As shown in Table 1, Hwange coal and pinus sawdust particles have different densities, for example, HC100 has a density of 1300 kg/m^3 and HC70PS30 has a density of 1030 kg/m^3. As explained by Gao et al. [24] during their studies with woodchip and Mandø et al. [40] during their studies with straw, biomass tends to assume a cylindrical shape when pulverised which increases its drag propensity when compared to a quasi-sphere pulverised coal particle. The HC100 fuel blend had a residence time of 0.81 s at a distance of 520 mm from the injection point as shown in Fig. 4. The aerodynamic factors of drag and gravitational acceleration within the DTF imply that the residence time for HC100 is mainly influenced by gravitational acceleration since HC100 has a larger density and hence weight when compared to the other blended samples. However, once pinus sawdust is blended, the residence time tends to be influenced by drag properties hence the trends displayed in Fig. 4 [24, 40].

Stage 2 residence times which represent the combustion of the char product obtained from stage 1 are represented in Figs. 5 and 6. The trends shown in Fig. 5 represent the effect of blending on residence time for a constant furnace temperature whilst Fig. 6 shows the

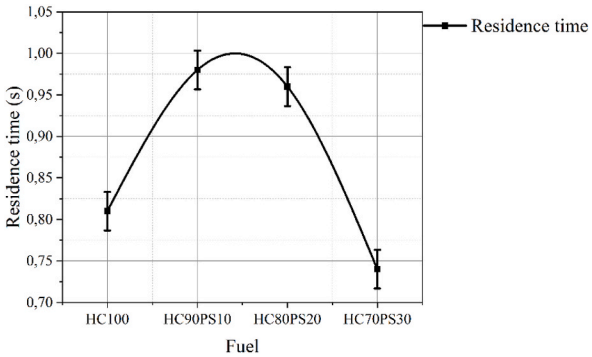

Fig. 4. DTF Stage 1 experimental particle residence times of HC100, HC90PS10, HC80PS20 and HC70PS30 fuel samples at 520 mm from the injection point.[5]

[5] HC: represents Hwange coal, PS: represents South African coal.

effect of furnace temperature (heating rate) on residence time. A decreasing trend of residence time with an increase in blending ratio was made apparent for all probing positions of 520, 920 and 1320 mm from the injection point. At a probing position of 1320 mm, the particle residence time decreased from 3.9 s to 2.0 s as blending by pinus sawdust increased from 0 to 30%. This trend was observed at all the probing positions when the furnace temperature was held constant, and the blending was varied. A decrease of 0.1 s in residence time can result in a significant decrease in burnout for coal combustion as highlighted by Abdul Jameel et al. [6]. Redha et al. [5] also highlighted that an increase of 2 s in residence time for biomass combustion will result in a maximum temperature decrease of 36 K. By studying the oxyfuel combustion of methane, Shakeel et al. [41] demonstrated that a decrease of 0.4 s in combustion residence time increases the carbon monoxide emissions by 9000 ppm. An et al. [42] investigated experimentally and through modelling the combustion of char from Rhenish lignite within a pressurised KIVAN drop tube reactor. Their findings showed that heavier particles

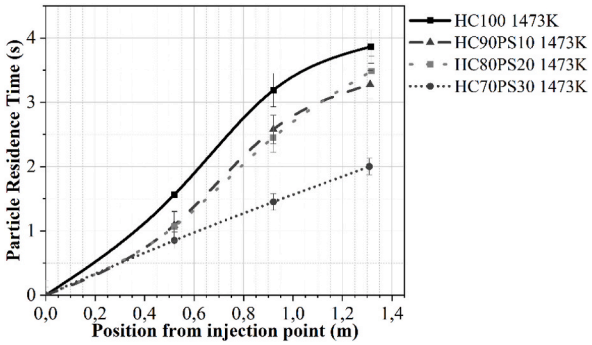

Fig. 5. DTF Stage 2 Plot of Experimental Residence Times of HC100, HC90PS10, HC80PS20 and HC70PS30 Fuel Samples at 1473 K furnace temperature.

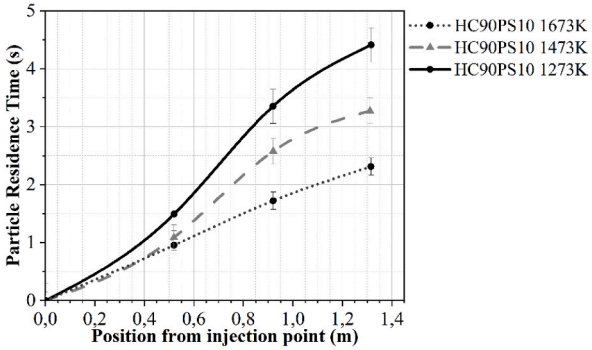

Fig. 6. DTF Stage 2 Plot of Experimental Residence Times of HC90PS10 Fuel Sample at 1273 K, 1473 K and 1673 K furnace temperature.

Table 4
DTF stage 2 experimental particle temperatures of SA coal sample.

s	Particle Temperature (K)		
	1273K	1473K	1673K
SA Coal (Exp) 520 mm	1248	1460	1677
SA Coal (Exp) 920 mm	1192	1412	1634
SA Coal (Exp) 1320 mm	1043	1276	1511

produce longer residence times than lighter particles hence agreeing with the results from this study as demonstrated in Table 1. Furthermore, as alluded to earlier, the cylindrical shape assumed by biomass increases the drag propensity of highly blended fuel samples [40,43].

The effect of heating rate as represented in Fig. 6 demonstrates how increasing the furnace temperature from 1273 to 1673 K influences the residence time for an HC90PS10 fuel sample. At a probing position of 1320 mm from the injection point, the residence time changed from 4.4 to 2.3 s which represents a 47.73% decrease over a temperature range of 400 K. Similar trends are exhibited at all probing positions highlighting the tremendous influence that the heating rate has on particle residence time. As demonstrated experimentally by Holmgren et al. [9], high heating rates result in a higher relative particle diameter and smaller relative density due to the rapid release of volatiles which hinder particle plasticization during devolatilisation or shrinkage of pores during char combustion. This phenomenon in turn leads to combustion particles appearing lighter making it easier for them to move quickly through the furnace, hence a decrease in residence time. Some researchers have gone further to investigate the effect of pressure as well as the combusting atmosphere on residence time with success [42].

4.2. Temperature profiles

As with residence time, the South African fuel sample was used to calibrate the DTF through monitoring of particle temperature for stage 2. The data presented in Table 4 and Fig. 7 is a summary of how the particle temperature varied under different heating rates for the SA coal sample. At a furnace wall temperature of 1673 K, the combusting particle attained an experimental temperature of 1677 K when probed at a distance of 520 mm from the injection point. The particle temperature decreased as the particle travelled through the DTF until attaining a temperature of 1511 K at a distance of 1320 mm from the injection point. All of the furnace temperature settings showed that generally, the fuel particle attained its maximum temperature at a location close to 520 mm from the injection point.

The fuels of interest, HC100, HC90PS10, HC80PS20, and HC70PS30 were thus investigated for both the influence of blending ratio as well as furnace temperature which closely resembles heating rate. As represented in Fig. 8, all blending ratios attain a similar temperature after a certain time within the furnace. For a furnace temperature of 1673 K and a residence time of 2.0 s, a particle temperature of 1719 K is attained by all these fuel blends. However, it is worth noting that these fuel blends attain a residence time of 2.0 s at different positions as explained earlier. The higher the blending ratio with pinus sawdust the easier it is for the fuel to travel within the furnace over a short period. This meant that the HC80PS20 fuel sample was able to attain a residence time of 2.0 s further downstream in the furnace than the HC100 fuel sample. Since the furnace wall temperature is isothermal (either at 1273, 1473 or 1673 K) and the fuel flow rates are small, the heat that is released from the fuel particles during the DTF combustion becomes too negligible to influence any change in wall temperature. This important deduction is also highlighted in the works done by An et al. [42] whilst studying solid fuel combustion in a pressurised DTF. They admitted that failure to achieve an isothermal wall temperature tends to result in non-homogenous temperature and velocity distributions which are difficult to analyse and employ for validation purposes.

In Fig. 9, the researchers investigated the effect of furnace temperature on particle temperature. It was made apparent that higher furnace temperatures are synonymous with higher particle temperatures, which was an expected outcome. At a residence time of 3.0 s, the HC80PS20 fuel sample attains a particle temperature of 1555 K for a furnace temperature of 1673K which is 26.12% higher than the 1233 K particle temperature obtained when the furnace is heated to 1273K.

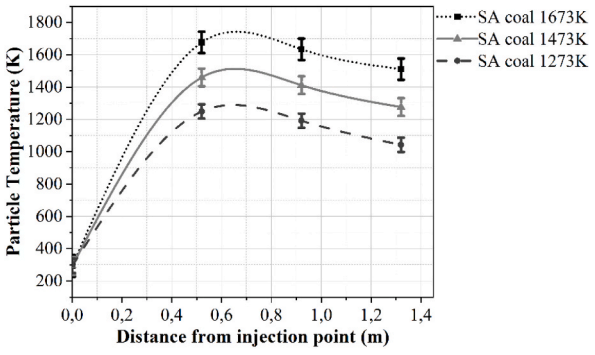

Fig. 7. DTF stage 2 plot of experimental particle temperatures of SA coal sample.

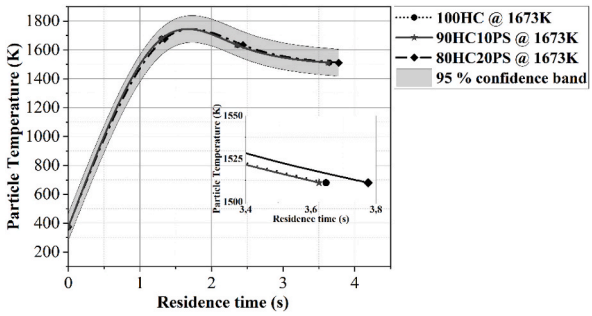

Fig. 8. DTF Stage 2 Plot of Experimental Particle Temperatures of HC100, HC90PS10, HC80PS20 and HC70PS30 Fuel Samples at 1673 K furnace temperature.

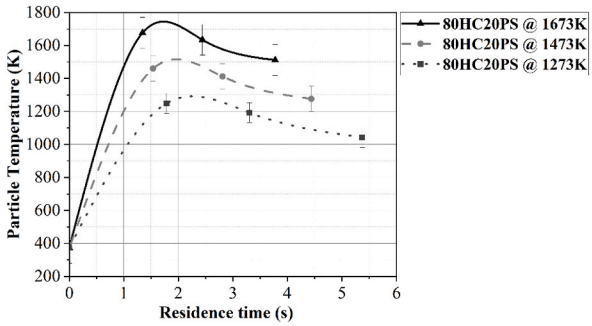

Fig. 9. DTF Stage 2 Plot of Experimental Particle Temperatures of HC80PS20 Fuel Sample at 1273 K, 1473 K and 1673 K furnace temperature.

4.3. Effect of blending on combustion parameters

Change in particle residence time due to blending has a direct effect on burnout, combustion stability and intensity. Indexes representative of these combustion parameters have been employed by a few researchers through the use of TGA experiments [1,44]. Unfortunately, since the residence times within the DTF are very short, it becomes difficult to determine these indexes since they are a function of mass loss rate which is difficult to measure at rapid mass loss percentages. Wang et al. [45] showed that blending increases the combustion intensity whilst decreasing combustion stability. Guan et al. [3] demonstrated that short residence times during combustion are synonymous with rapid release of volatiles, a major contributor to combustion stability [1]. As such, due to the drop in residence time exhibited by the fuel samples as the blending increases from 0 to 30 %, Figs. 5 and 4, combustion becomes less stable.

Due to the low fuel flow rates employed in this study, the effect of blending on particle temperature could not be made apparent, an important parameter that should be used to deduce changes in ignition and burnout properties of combusting samples. An increase in particle temperature results in increased ignition and burnout properties of fuel samples. This is because all of the elementary reactions between carbon, oxygen and carbon monoxide have the highest efficiency after the release of volatiles which is within a temperature range of 673 and 823 K [46]. At high furnace temperatures, Fig. 9 shows that fuel particles can attain higher particle temperatures. Most researchers employ the rate of particle mass loss to determine ignition and burnout indexes [47]. However, Haykiri-Acma et al. [35] made it apparent that the rate of particle mass loss is mainly influenced by particle temperature. As such this study was able to highlight the trends in particle temperature as furnace temperature increases and blending by pinus sawdust increased.

5. Conclusions

The influence of blending Hwange coal with pinus sawdust was experimentally investigated through the use of a DTF. The input variables that were investigated were blending ratio, distance from the injection point as well as furnace temperature to mimic the heating rate a combusting particle goes through. The following conclusions were derived from this research.

- During stage 1 of the experimental setup, particle residence time at a distance of 520 mm from the injection point decreased from 0.8 to 0.7 s as blending by pinus sawdust increased from 0 to 30 %. Similarly, during stage 2 of the experimental setup, particle residence time at a distance of 1320 mm from the injection point decreased from 3.9 to 2.0 s as blending by pinus sawdust increased from 0 to 30 %. This was attributed to the increase in drag which meant that highly blended samples could be carried with less effort along the furnace. Varying the furnace wall temperature between 1273 K, 1473 K and 1673 K and measuring the particle residence time at a distance of 1320 mm from the injection point showed a decrease in particle residence time from 4.4 to 2.3 s for the fuel

blend with 90% Hwange coal and 10% pinus sawdust. The blending ratios under investigation, 0%, 10%, 20%, and 30% pinus sawdust by mass substitution, demonstrated similar profiles of particle temperature at different furnace positions though further analysis showed that the highly blended samples required less time to attain high temperatures.

- This study thus highlights to combustion engineers how blending coal and pinus sawdust results in a change of particle residence time. Fuel blends with higher percentages of pinus sawdust exhibited shorter residence time which meant the particles moved through the furnace more quickly, hence combustion stability is decreased.
- This study also made it apparent how blending coal with pinus sawdust results in a change of particle temperature. Fuel blends with higher percentages of pinus sawdust were able to attain higher temperatures over a shorter residence time which meant combustion intensity increased with blending ratio. As such, since the high temperature zones moved backwards towards the fuel injection point, burner modification will be required for highly blended samples.
- Various limitations were experienced within this study. The most prominent one was due to the poor particle collection efficiency at the furnace outlet. As such, further studies that employ cyclones or electrostatic filters with higher collection efficiencies should be carried out. Further design modifications to the existing DTF should also be done so more combustion data is generated. This includes the installation of visualisation ports, increasing probing positions and use of measuring instruments and furnace materials that can handle a larger range of carrier gasses. In as much as the fuel particles were analysed by use of sieve analysis, further studies which employ scanning electron microscopy analysis will need to be carried out. This can give a better understanding of the aerodynamic properties exhibited during combustion through understanding of fuel particle sphericity.

In summary, all the objectives set out in this research were archived which gave the researchers important data that can be used for co-combustion modelling through validation of experimental data.

Data availability statement

Data associated with this study has not been deposited into a publicly available repository because the data is included as supplementary material that is published alongside the article.

CRediT authorship contribution statement

Garikai T. Marangwanda: Writing – review & editing, Writing – original draft, Visualization, Validation, Methodology, Investigation, Formal analysis, Conceptualization. **Daniel M. Madyira:** Writing – review & editing, Supervision, Resources, Project administration, Funding acquisition.

Declaration of competing interest

The authors declare the following financial interests/personal relationships which may be considered as potential competing interests: None.

Acknowledgements

Special thanks to the University of Johannesburg, South Africa, for supporting the authors during this research.

Appendix A. Supplementary data

Supplementary data to this article can be found online at https://doi.org/10.1016/j.heliyon.2024.e27287.

- (Fig. S1) - (Fig. S3): DTF Stage 2 Plot of Experimental Residence Times of HC90PS10, HC80PS20, HC70PS30 Fuel Sample at 1273 K, 1473 K and 1673 K furnace temperature.
- (Fig. S4) - (Fig. S6): DTF Stage 2 Plot of Experimental Residence Times of HC90PS10, HC80PS20 and HC70PS30 Fuel Samples at 1673 K furnace temperature.
- (Fig. S7) - (Fig. S9): DTF Stage 2 Plot of Experimental Particle Temperatures of HC100, HC90PS10, HC80PS20 Fuel Sample at 1273 K, 1473 K and 1673 K furnace temperature.

References

[1] G.T. Marangwanda, D.M. Madyira, P.G. Ndungu, C.H. Chihobo, Combustion characterisation of bituminous coal and pinus sawdust blends by use of thermogravimetric analysis, Energies 14 (2021) 1–20, https://doi.org/10.3390/en14227547.

[2] J. Ju, X. Duan, B. Sarkodie, Y. Hu, H. Jiang, C. Li, Numerical simulation of flow field and residence time of nanoparticles in a 1000-ton industrial multi-jet combustion reactor, Chin. J. Chem. Eng. 51 (2022) 86–99, https://doi.org/10.1016/j.cjche.2021.12.008.

[3] J. Guan, Q. Yu, G. Zuo, M. Wang, W. Li, G. Wang, Z. Pang, Characteristics of volatile release rate and fuel nitrogen conversion for three typical coals under high temperature fast pyrolysis, IOP Conf. Ser. Earth Environ. Sci. 227 (2019) 042049, https://doi.org/10.1088/1755-1315/227/4/042049.

[4] H. Haykiri-Acma, S. Yaman, Synergistic investigation for co-combustion of biochars and lignite-thermogravimetric analysis approach, J. Therm. Sci. Eng. Appl. 11 (2019), https://doi.org/10.1115/1.4040992.

[5] A. Mohammed Redha, A. Lau, M. Holuszko, A. Vakil, S. Sokhansanj, CFD investigation of pelletization effect on co-firing coal with wheat straw, Can. J. Chem. Eng. 100 (2022) 237–253, https://doi.org/10.1002/cjce.24106.

[6] A.G. Abdul Jameel, C. Dahiphale, A.B.S.S. Alquaity, U. Zahid, S. Jayanti, Numerical simulation of coal combustion in a tangential pulverized boiler: effect of burner vertical tilt angle, Arabian J. Sci. Eng. (2021), https://doi.org/10.1007/s13369-021-05613-8.

[7] D. Zabrodiec, A. Massmeyer, J. Hees, O. Hatzfeld, R. Kneer, Flow pattern and behavior of 40 kWth pulverized torrefied biomass flames under atmospheric and oxy-fuel conditions, Renew. Sustain. Energy Rev. 138 (2021) 110493, https://doi.org/10.1016/j.rser.2020.110493.

[8] B.N. Madanayake, S. Gan, C. Eastwick, H.K. Ng, An investigation into the use of CFD to model the co-firing of Jatropha curcas seed cake with coal, Int. J. Green Energy 15 (2018) 605–621, https://doi.org/10.1080/15435075.2018.1525559.

[9] P. Holmgren, D.R. Wagner, A. Strandberg, R. Molinder, H. Wiinikka, K. Umeki, M. Broström, Size, shape, and density changes of biomass particles during rapid devolatilization, Fuel 206 (2017) 342–351, https://doi.org/10.1016/j.fuel.2017.06.009.

[10] L. Ma, M. Gharebaghi, R. Porter, M. Pourkashanian, J.M. Jones, A. Williams, Modelling methods for co-fired pulverised fuel furnaces, Fuel 88 (2009) 2448–2454, https://doi.org/10.1016/j.fuel.2009.02.030.

[11] P. Graeser, M. Schiemann, Investigations on the emissivity of burning coal char particles: influence of particle temperature and composition of reaction atmosphere, Fuel 263 (2020) 116714, https://doi.org/10.1016/j.fuel.2019.116714.

[12] G.T. Marangwanda, D.M. Madyira, T.O. Babarinde, Coal combustion models: a review, J. Phys. Conf. Ser. 1378 (2019) 032070, https://doi.org/10.1088/1742-6596/1378/3/032070.

[13] S. Su, J. Pohl, D. Holcombe, J. Hart, Techniques to determine ignition, flame stability and burnout of blended coals in p.f. power station boilers, Prog. Energy Combust. Sci. 27 (2001) 75–98, https://doi.org/10.1016/S0360-1285(00)00006-X.

[14] A.C. Sarroza, T.D. Bennet, C. Eastwick, H. Liu, Characterising pulverised fuel ignition in a visual drop tube furnace by use of a high-speed imaging technique, Fuel Process. Technol. 157 (2017) 1–11, https://doi.org/10.1016/j.fuproc.2016.11.002.

[15] C. Wang, Y. Zhang, P. Wang, J. Zhang, Y. Du, D. Che, Effects of silicoaluminate oxide and coal blending on combustion behaviors and kinetics of zhundong coal under oxy-fuel condition, J. Therm. Anal. Calorim. 134 (2018) 1975–1986, https://doi.org/10.1007/s10973-018-7627-7.

[16] X. Xing, S. Wang, Q. Zhang, Thermogravimetric analysis and kinetics of mixed combustion of waste plastics and semicoke, J. Chem. 2019 (2019) 10, https://doi.org/10.1155/2019/8675986.

[17] D.E. Priyanto, Y. Matsunaga, S. Ueno, H. Kasai, T. Tanoue, K. Mae, H. Fukushima, Co-firing high ratio of woody biomass with coal in a 150-MW class pulverized coal boiler: properties of the initial deposits and their effect on tube corrosion, Fuel 208 (2017) 714–721, https://doi.org/10.1016/j.fuel.2017.07.053.

[18] A.H. Al-Abbas, J. Naser, Effect of chemical reaction mechanisms and NOx modeling on air-fired and oxy-fuel combustion of lignite in a 100-kW furnace, Energy Fuel. 26 (2012) 3329–3348, https://doi.org/10.1021/ef300403a.

[19] C. Yin, L.A. Rosendahl, T.J. Condra, S.K. Kær, Use of numerical modeling in design for co-firing biomass in wall-fired burners, Chem. Eng. Sci. 59 (2004) 3281–3292, https://doi.org/10.1016/j.ces.2004.04.036.

[20] J. Deng, B. Li, Y. Xiao, L. Ma, C.P. Wang, B. Lai-wang, C.M. Shu, Combustion properties of coal gangue using thermogravimetry–Fourier transform infrared spectroscopy, Appl. Therm. Eng. 116 (2017) 244–252, https://doi.org/10.1016/j.applthermaleng.2017.01.083.

[21] K. Savolainen, Co-firing of biomass in coal-fired utility boilers, Appl. Energy 74 (2003) 369–381, https://doi.org/10.1016/S0306-2619(02)00193-9.

[22] H. Rüdiger, A. Kicherer, U. Greul, H. Spliethoff, K.R.G. Hein, Investigations in combined combustion of biomass and coal in power plant technology, Energy Fuel. 10 (1996) 789–796, https://doi.org/10.1021/ef950222w.

[23] H. Kruczek, P. Rczka, A. Tatarek, The effect of biomass on pollutant emission and burnout in co-combustion with coal, Combust. Sci. Technol. 178 (2006) 1511–1539, https://doi.org/10.1080/00102200600721297.

[24] F. Guo, Y. He, A. Hassanpour, J. Gardy, Z. Zhong, Thermogravimetric analysis on the co-combustion of biomass pellets with lignite and bituminous coal, Energy 197 (2020) 1–9, https://doi.org/10.1016/j.energy.2020.117147.

[25] R. Pérez-Jeldres, P. Cornejo, M. Flores, A. Gordon, X. García, A modeling approach to co-firing biomass/coal blends in pulverized coal utility boilers: synergistic effects and emissions profiles, Energy 120 (2017) 663–674, https://doi.org/10.1016/j.energy.2016.11.116.

[26] A.A. Bhuiyan, A.S. Blicblau, J. Naser, Co-firing of biomass and slagging in industrial furnace: a review on modelling approach, J. Energy Inst. 90 (2017) 838–854, https://doi.org/10.1016/j.joei.2016.08.010.

[27] M. Mureddu, F. Dessì, A. Orsini, F. Ferrara, A. Pettinau, Air-and oxygen-blown characterization of coal and biomass by thermogravimetric analysis, Fuel 212 (2018) 626–637, https://doi.org/10.1016/j.fuel.2017.10.005.

[28] J. Wnorowska, S. Ciukaj, S. Kalisz, Thermogravimetric analysis of solid biofuels with additive under air atmosphere, Energies 14 (2021) 2257, https://doi.org/10.3390/en14082257.

[29] X. Jiang, C. Wang, X. Wang, Y. Liu, Z. Song, Q. Lin, Co-combustion of coal and carbonaceous wastes: thermogravimetric analysis, Energy Sources, Part A Recover, Util. Environ. Eff. 00 (2020) 1–15, https://doi.org/10.1080/15567036.2019.1704314.

[30] C. Baukal Jr., Industrial Combustion Pollution and Control, CRC Press, 2003, https://doi.org/10.1201/9780203912782.

[31] J. Colannino, Modeling of Combustion Systems, first ed., CRC Press, 2006 https://doi.org/10.1201/9781420005035.

[32] L. Chen, S.Z. Yong, A.F. Ghoniem, Oxy-fuel combustion of pulverized coal: characterization, fundamentals, stabilization and CFD modeling, Prog. Energy Combust. Sci. 38 (2012) 156–214, https://doi.org/10.1016/j.pecs.2011.09.003.

[33] P. Ayazi Shamlou, Processing of Solid–Liquid Suspensions, first ed., Butterworth-Heinemann, 1993 https://doi.org/10.1016/C2013-0-04585-9.

[34] G.T. Marangwanda, D.M. Madyira, C.H. Chihobo, Determination of cocombustion kinetic parameters for bituminous coal and pinus sawdust blends, ACS Omega 7 (2022) 32108–32118, https://doi.org/10.1021/acsomega.2c03342.

[35] H. Haykiri-Acma, A. Baykan, S. Yaman, S. Kucukbayrak, Are medium range temperatures in Drop Tube Furnace really ineffective? Fuel 105 (2013) 338–344, https://doi.org/10.1016/j.fuel.2012.05.008.

[36] R. Khatami, C. Stivers, Y.A. Levendis, Ignition characteristics of single coal particles from three different ranks in O2/N2 and O2/CO2 atmospheres, Combust. Flame 159 (2012) 3554–3568, https://doi.org/10.1016/j.combustflame.2012.06.019.

[37] H.K. Versteeg, W. Malalasekera, An Introduction to Computational Fluid Dynamics: the Finite Volume Method Approach, Prentice Hall, 1996, 9780582218840.

[38] S. Turns, An Introduction to Combustion: Concepts and Applications, second ed., McGraw-Hill, New York, 1996. https://books.google.co.za/books?id=c6qUCgAAQBAJ. accessed June 9, 2020.

[39] T. Katarzyna, S. Stęchły, CFD Modelling of Pulverised Coal and Biomass Combustion, 2019.

[40] M. Mandø, L.A. Rosendahl, C. Yin, H. Sørensen, Pulverized straw combustion in a low-NOx multifuel burner: modeling the transition from coal to straw, Fuel 89 (2010) 3051–3062, https://doi.org/10.1016/j.fuel.2010.05.016.

[41] M.R. Shakeel, Y.S. Sanusi, E.M.A. Mokheimer, Numerical modeling of oxy-methane combustion in a model gas turbine combustor, Appl. Energy 228 (2018) 68–81, https://doi.org/10.1016/j.apenergy.2018.06.071.

[42] F. An, Z. Dai, S. Guhl, M. Gräbner, A. Richter, Detailed analysis of the particle residence time distribution in a pressurized drop-tube reactor, AIChE J. 69 (2023) 1–13, https://doi.org/10.1002/aic.18026.

[43] H. Gao, A. Runstedtler, A. Majeski, P. Boisvert, D. Campbell, Optimizing a woodchip and coal co-firing retrofit for a power utility boiler using CFD, Biomass Bioenergy 88 (2016) 35–42, https://doi.org/10.1016/j.biombioe.2016.03.006.

[44] S.P. Bermejo, A. Prado-guerra, A. Isabel, P. García, L. Fernando, C. Prieto, Study of quinoa plant residues as a way to produce energy through thermogravimetric analysis and indexes estimation, Renew. Energy 146 (2020) 2224–2233, https://doi.org/10.1016/j.renene.2019.08.056.

[45] R. Wang, Z. Liu, X. Song, S. Liu, Co-combustion of pulverized coal and walnut shells in air and oxy-fuel atmospheres: thermal behavior, synergistic effect and kinetics, J. Energy Inst. 108 (2023) 101243, https://doi.org/10.1016/j.joei.2023.101243.
[46] W. Zhou, H. Huo, Q. Li, R. Dou, X. Liu, An improved comprehensive model of pyrolysis of large coal particles to predict temperature variation and volatile component yields, Energies 12 (2019) 884, https://doi.org/10.3390/en12050884.
[47] H.F. Lü, J. Deng, D.J. Li, F. Xu, Y. Xiao, C.M. Shu, Effect of oxidation temperature and oxygen concentration on macro characteristics of pre-oxidised coal spontaneous combustion process, Energy 227 (2021) 120431, https://doi.org/10.1016/j.energy.2021.120431.